D_p = particle diameter (mm.)
ϵ = external void fraction (ml. fluid/ml. packed volume)
f = internal void fraction (ml. fluid/ml. packed volume)
K_d = equilibrium distribution coefficient (dimensionless)
k = mass transfer coefficient (min.$^{-1}$)
L = solution flow rate [ml./(min.)(sq.cm.)]
q = solute concentration in internal solution (milli-equivalents/ml.)
q_i = initial solute concentration within the bed
q_o^* = internal concentration in equilibrium with external concentration C_o
t = time (min.)
V_{int} = total particle internal volume (ml.)
Z = axial distance in bed (cm.)

LITERATURE CITED

1. Asher, D., and D. W. Simpson, *J. Phys. Chem.*, **60**, 518 (1956).
2. Furnas, C. C., *Bureau of Mines Bulletin 361* (1932).
3. Gilliland, E. R., and R. F. Baddour, *Ind. Eng. Chem.*, **45**, 330 (1953).
4. Hiester, N. K., and Theodore Vermeulen, *Chem. Eng. Progr.*, **48**, 505 (1952).
5. Hougen, O. A., and K. M. Watson, "Chemical Process Principles," Vol. 3, Wiley, New York (1947).
6. Kunin, Robert, "Ion Exchange Resins," 2 ed., p. 14, Wiley, New York (1958).
7. Miner, C. S., and N. N. Dalton, "Glycerol," Reinhold, New York (1953).
8. Nachod, F. C., and J. A. Schubert, "Ion Exchange Technology," Chap. 7, Academic Press, New York (1956).
9. *Ibid.*, p. 190.
10. Opler, A., and N. K. Hiester, "Tables for Predicting the Performance of Fixed Bed Ion Exchange and Similar Mass Transfer Processes," Stanford Research Institute, Stanford, California (1954).
11. Prielipp, C., and M. Keller, *Am. Oil Ch. S. Journal*, **33**, 103 (1956).
12. Schuman, T. E., *J. Franklin Inst.*, **208**, 405 (1929).
13. Shurts, E. L., and R. R. White, *A.I.Ch. E. Journal*, **3**, 183 (1957).
14. Simpson, D. W., and R. M. Wheaton, *Chem. Eng. Progr.*, **50**, 45 (1954).
15. Simpson, D. W., and W. C. Bauman, *Ind. Eng. Chem.*, **46**, 1958 (1954).
16. Tayyabkhan, M. T., Ph.D. dissertation, Univ. Michigan, Ann Arbor, Michigan (1959).
17. Vassiliou, Basil, Thesis, National Technical University of Athens, Greece (1957).
18. Vermeulen, Theodore, "Advances in Chemical Engineering," Vol. 2, p. 147, *Academic Press*, New York (1958).
19. ———, and N. K. Hiester, *Ind. Eng. Chem.*, **44**, 636 (1952).
20. Wheaton, R. M., and W. C. Bauman, *ibid.*, **45**, 228 (1953).

Manuscript received June 13, 1961; revision received October 17, 1961; paper accepted October 18, 1961. Paper presented at A.I.Ch.E. Lake Placid meeting.

Fundamental Aspects of Rotating Disk Contactor Performance

C. P. STRAND, R. B. OLNEY, and G. H. ACKERMAN

Shell Development Company, Emeryville, California

The principles used in analyzing the performance of rotating disk contactor liquid extraction columns are discussed. The behavior of a swarm of drops in the rotating field is found to be adequately represented in most respects by single-drop dynamics, which leads to tested relations for countercurrent capacity, limiting drop holdup, axial diffusion of the continuous and dispersed phases, and point mass transfer coefficients that are independent of column size effects.

The rotating disk contactor (RDC) was introduced several years ago (*20*) and has been applied successfully in a number of liquid-liquid extraction applications. These include lube oil and gas oil extractions, propane deasphalting, sulfur dioxide extraction of kerosene fractions, solutizer treating, recovery of phenol from effluents, extraction of catalytic reformates, and miscellaneous chemicals and specialties applications. Various data for this device have been published (*5, 13, 16, 20, 22, 32*), but a comprehensive analysis of all such data has not been presented heretofore. The present work is an attempt to do this, with first principles wherever possible. The intent is to show the extent to which these principles have been verified and to outline the design philosophy that has evolved, without going into the details of the design procedure. The important assumptions and limitations are illustrated, and the concepts that require further study and verification are mentioned. The methods have been used to achieve a successful scale-up in several cases.

The RDC consists of a number of rotating disks supported on a shaft, the disks being centered between stator rings which form the compartments (*20*). A sketch of the apparatus is shown in Figure 1. The variables that must be selected for a design include the column diameter, the rotor disk diameter, the rotational speed, the diameter of the stator opening, the compartment height, and the number of compartments. When two immiscible phases are present, in countercurrent extraction, then the drop size and the amount of the drop phase in the contact zone are governed mainly by the rotor speed. A low speed results in large drops which rise rapidly through the contact zone, thereby permitting high throughputs but giving small interfacial areas and low mass transfer rates. A high rotor speed gives very small approximately spherical drops which revolve many times within a compartment along toroidal paths. This leads to lower column capacity but gives high mass transfer rates because of the increased interfacial area.

In addition to increasing the dispersed-phase holdup and the interfacial area an increase in rotor speed causes an increase in axial mixing of each phase. The two main components of the axial diffusion process are an eddy diffusion or backmixing, most pronounced at highest speeds, and a channeling or Taylor type of diffusion (*27*) which is specific in the forward direction. Axial mixing, when present

in both phases, clearly causes a reduction in the concentration driving force between the phases. This competes with the local transfer conditions around a drop, in determining the over-all or effective mass transfer rate. Higher rotor speed increases the local or true transfer rate, but ultimately this is offset by increased axial mixing; therefore one may anticipate an optimum rotor speed for each operating condition. Stated another way, variable speed imparts flexibility to a design by permitting the selection of conditions for best column efficiency, for a range of flow rates and phase ratios.

It has long been known that a point efficiency must be corrected for the effect of flow imperfections in an apparatus, in order to arrive at the over-all efficiency. Unfortunately, assured procedures for doing this are not yet available for most types of two-phase contactors. To cite a case, large diameter spray columns are less efficient than small ones, but reliable methods for translating from one scale to another have not been published. The information given here is a convincing demonstration of the separation of point transfer effects and gross flow effects in an extraction device.

The equipment dimensions, the liquid systems used, and the phenomena studied in the several investigations reviewed here are itemized in Table 1. Feed and solvent phases are referred to in the text, figures and tables; solute is extracted from the feed phase to the solvent phase in all cases.

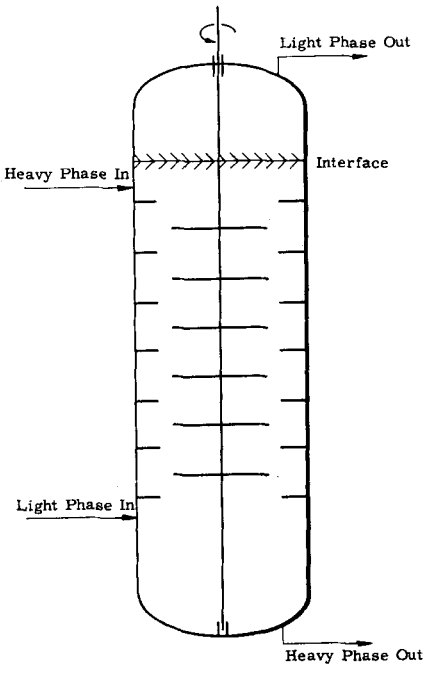

Fig. 1. Rotating disk contactor illustrated for operation with light phase dispersed.

DROP SIZE

Hinze (7) has proposed an equation for maximum stable drop size, based on the assumption of an isotropic homogeneous turbulence and where the microscale of the turbulence is smaller than the drop size (12):

$$d_m = C_1 \left(\frac{g_c \sigma}{\rho_c} \right)^{3/5} \epsilon^{-2/5} \qquad (1)$$

He has reported the constant C_1 to be about 0.72, based on an analysis of the rotating cylinder data of Clay (4). However, as indicated by Sleicher (25), neither an exponent of $-2/5$ on ϵ nor a value of $C_1 = 0.72$ provides the best fit of the Clay data. Nevertheless the Hinze equation, with adjustment of the constant C_1 as necessary, has been used with some success for predicting d_{max} in certain devices such as globe valves, stirred tanks, and rotating cylinders; the explanation may be that the conditions for local isotropy to exist are met approximately. Moreover Vermeulen, Williams, and Langlois (31), Calderbank (3), and Kafarov and Babanov (11) have been successful in correlating mean drop sizes in stirred tanks using equations of this form. Further, the data of Clay (4) suggest that, as a first approximation, the ratio, mean drop size/maximum drop size, may be taken as a constant. This has encouraged the authors to use Equation (1) to predict average drop sizes in the present analysis, where the coefficient C_1 is adjusted to match the specific conditions accompanying mass transfer, tendency of drops to coalesce, and the like. A refinement of this analysis would, of course, demand a more rigorous approach to the problem of drop breakup in stirred systems.

TABLE 1. SUMMARY OF RDC STUDIES

Reference	Liquid systems	Measurements	Unit	Column dimensions D, in.	L, ft.	S/D	R/D	H/D
(16)	Toluene-acetone-water	Holdup, capacity, mass transfer	a	3	2	0.667	0.500	0.333
	Butyl acetate-acetone-water		b	3	2	0.750	0.500	0.333
	Toluene-water		c	3	2	0.750	0.500	0.500
	Butyl acetate-water		d	3	2	0.750	0.500	0.167
	Isooctane-water		e	3	2	0.750	0.500	0.667
	Benzene-water		f	3	2	0.750	0.333	0.333
	White spirit-water		g	3	2	0.750	0.667	0.333
			h	3	2	0.750	0.333	0.333
			k	3	2	0.750	0.500	1.333
(32)	MIBK-acetic acid-water	Holdup, capacity, mass transfer	i	1.6	1.55	0.760	0.490	0.490
(20) and present inv.	Kerosene-NBA-water	Holdup, capacity, mass transfer	l	4	4	0.750	0.500	0.500
			m	16	4	0.750	0.500	0.500
			n	16	4	0.750	0.500	0.375
			o	16	4	0.750	0.500	0.250
			p	16	2	0.750	0.500	0.250
			q	16	4	0.750	0.500	0.150
			r	16	4	0.750	0.625	0.250
			s	16	4	0.750	0.719	0.250
			t	16	4	0.648	0.625	0.250
(20) and present	MIBK-acetic acid-water	Holdup, mass transfer	j	4	4	0.750	0.500	0.500
Present inv.	Toluene-acetone-water	Holdup, maximum drop size, capacity, axial mixing, mass transfer, mixing times	u	6	5.95	0.667	0.500	0.349
	Toluene-MEK-water		v	41.5	10	0.783	0.505	0.241
	Toluene-water (see Table 2 for systems used in drop size studies)							

TABLE 2. SYSTEMS USED IN STUDY OF MAXIMUM STABLE DROP SIZE

	Dispersed phase	Continuous phase
(a)	Toluene	Water
(b)	Water	Toluene
(c)	Toluene	60% glycerine/40% water
(d)	Butyl acetate	Water
(e)	37% kerosene/63% CCl_4	Water
(f)	68% kerosene/32% CCl_4	Water
(g)	Water	82% kerosene/18% CCl_4
(h)	Water	37% kerosene/63% CCl_4
(i)	White oil	Water

An illustration of the application of the Hinze equation for drop breakup in an RDC is provided by some experiments to determine maximum stable drop size in the 6-in. diam. unit (unit u, Table 1). Values of d_m were estimated from replicate photographs of about 3.8X magnification. The pictures were taken through the glass wall of the column at an exposure of 0.001 sec.; the area photographed was about 2 in. × 2 in., and the focus was about ½ in. inside the column wall. The camera station was at a position twenty-three or twenty-four compartments removed from the dispersed-phase inlet to provide conditions favorable for forming an equilibrium drop distribution. In selecting a value of d_m from each photograph the authors neglected those largest drops that were obviously coalescing or breaking up and those for which the major/minor axis ratio was greater than about 1.3. Drop holdup (in the range 5 to 20%) and drop residence time appeared to have not much effect on the results and, accordingly, are not reported. Table 2 lists the liquid pairs studied; Figure 2 shows the original data plotted as a function of rotor speed, and Figure 3 shows a comparison between the data and equation (1). Here, and elsewhere throughout the paper, the power/mass is defined as

$$\epsilon = \frac{4}{\pi} C_2 \frac{N^3 R^5}{HD^2} \qquad (2)$$

where C_2 is the coefficient in the power number (21)

$$\frac{P}{n\rho N^3 R^5} = C_2 \qquad (3)$$

It is seen that the data with the organic phase dispersed fall approximately in the range $C_1 = 0.4$ to 0.6, although the effect of ϵ is somewhat greater than that given by an exponent of −2/5. The worst agreement with $d_m \sim \epsilon^{-2/5}$ is found with system *i*, which is the only case where the drops are very viscous (oil viscosity 26 centipoises). In contrast, runs with aqueous phase dispersed (systems *b*, *g*, and *h*, Table 2) show considerably larger drop sizes, probably explained by the greater tendency of aqueous drops to coalesce readily and to adhere to the column surfaces. The agreement with the mechanism generally is poorest at the lower rotor speeds in each series of runs, which is not surprising since the conditions for local isotropy to exist are less likely when the speed is low and the drop size and drop settling velocity are large.

It may be that both the boundary layer shear mechanism proposed by Sleicher (25) and the Hinze mechanism govern the breakup of noninteracting drop systems in an RDC. This could explain the greater effect of rotor speed on drop size then predicted by Equation (1).

Some attempts to measure d_m during mass transfer studies have been made, with the same photographic technique. The authors have not obtained enough information to generalize, but it can be said that such data will be more difficult to interpret, especially if the rates of drop breakup or drop coalescence are sensitively affected by solute concentration or by the direction of transfer. Distinctly larger drops throughout the column have been seen in one case, evidence that drop breakup is delayed by the presence of solute was found with another system, and a region of considerably smaller drops over a few compartments was seen in another case. In each case the effects found probably are specific for the column length, mass transfer rate, and solute concentration used.

These observations suggest that a mechanism for predicting d or d_m during mass transfer will be difficult to devise. Fortunately, an indirect method is available which gives a value of d that is satisfactory for most correlations of RDC capacity and efficiency data. In this procedure, which is described later, the drop velocity u is calculated with the appropriate measured drop holdup, and a characteristic diameter d is estimated from u and an appropriate drop settling curve. This procedure, with guidance supplied by the d_m correlation for nontransferring systems just described, has worked satisfactorily in several scale-up studies.

HOLDUP MEASUREMENTS

The drop holdup enters into a number of relations for capacity and mass transfer rate that are discussed in later paragraphs. Only the average value of h has been determined in some of the authors' studies and in those of others (*13, 16, 32*), but in certain other studies the authors have determined point values of h from two-phase samples drawn through probes located at various points along the column length. In one study, with the toluene-water system in 6- and 42-in. diameter RDC's, a detailed description of the radial and axial variations in h was obtained. Figures 4 and 5 give illustrative data for toluene dispersed in water in the 42-in. unit and for one flow rate and several rotor speeds. The results obtained at other flow rates are qualitatively similar. Also, similar results were found in the 6-in. unit except that the radial profiles in that unit were more erratic, possibly a result of the small dimensions.

Figure 4 shows the axial profiles for a position 4 in. in from the column wall (the stator rings extend in another ½ in. beyond this point). Data are given for positions 2½ in. above and 2½ in. below the stator rings, for compartments 1, 3, 6, 9, and 12, numbered above the toluene inlet. The holdup first increases, moving up the column, probably because a finite time is required for drop breakup. The decrease in h toward the top of the column may be due to the competing effects of axial diffusion of drops in the contact zone and of drop discharge into the sink provided by the internal settler located above the top stator ring. The run at 170 rev./min. is close to flooding, which apparently begins in the first few compartments.

The radial profiles of holdup in compartment 9 are shown in Figure 5. The holdup is essentially constant over most of the cross section but increases in the vicinity of the central rotor shaft, indicating some centrifugation of the light, dispersed phase. With water dispersed, data not shown, the profiles indicate the essential absence of water drops close to the center shaft.

From these and similar data the authors conclude that the appropriate value of h to use in determining the characteristic u and d for capacity and efficiency correlations is measured at a radial distance which is between $R/2$ and $S/2$ from the centerline and at the axial position that gives about the maximum value of h (runs at flooding have to be treated on an individual basis). Capacity and efficiency data for the toluene-water system in the 6- and 42-in. diameter

units have been treated in this way. Only average values of h are available for the other liquid systems considered here; however for cases studied in detail $(h)_{av}$ does not differ very much from $(h)_{max}$ except at low rotor speeds.

The effect of acetone transfer on the axial variation in h was determined, since data for the toluene-water-acetone system are an important part of the mass transfer analysis given here. Table 3* gives such holdup data, obtained in the 6-in. diameter RDC; they show that acetone transfer from toluene drops to water apparently has little effect on h. The same conclusion is reached later from a comparison of plots of u vs. ϵ for this system. On the other hand visual observations give the impression that the drops are larger when acetone transfer is occurring, and the data of Logsdail, Thornton, and Pratt (*16*) indicate that drop velocity is higher when acetone is being transferred. Some possible explanations for these differences are offered later.

Logsdail, et al. (*16*) have used h to calculate a drop velocity which is then correlated by a relation obtained by dimensional analysis, and Kung and Beckmann (*13*), in analyzing their holdup data for several RDC geometries, have followed the same procedure. The authors have preferred instead to try to devise a drop breakup mechanism that will explain the observed values of h; this work is described in the next section.

CAPACITY AND HOLDUP RELATIONS

The authors assume a relation for the characteristic drop velocity uC_R of the form proposed by Thornton (*28*) which should best apply when drop coalescence is not very important:

$$u = \frac{1}{C_R(1-h)}\left[\frac{V_d}{h} + \frac{V_c}{1-h}\right] \quad (4)$$

The drop holdup is determined experimentally, and the constriction factor is taken to be the minimum of the three area ratios

$$\left(\frac{S}{D}\right)^2, 1-\left(\frac{R}{D}\right)^2, \text{or} \left(\frac{S+R}{D}\right)\sqrt{\left(\frac{S-R}{D}\right)^2+\left(\frac{H}{D}\right)^2} \quad (5)$$

for the RDC in question. Velocity is related to the drop size by a drop settling relation obtained from the work of several investigators (*8, 9, 15*). It is assumed that the ratio d/d_{max} is approximately constant. A test of the procedure is provided by comparing calculated curves of u vs. ϵ [Equation (1), d/d_{max} = constant, and drop settling relation] with experimental values [Equations (4) and (5)]. Data for a given liquid system but for different column dimensions D, S, R, and H, rotor speeds, and flow rates V_d and V_c should fall on a single curve if the procedure is valid. This should hold for all values of h (including those at flooding), but the agreement may be poor at very small values of h, in view of the term V_d/h in Equation (4).

Also, following Thornton (*28*), the authors assume that the appropriate relation between the holdup at flooding h_f and the phase ratio V_c/V_d is obtained by setting the derivatives $(\partial V_c/\partial h)_{V_d}$ and $(\partial V_d/\partial h)_{V_c}$ of Equation (4) equal to zero; from the resulting equations one obtains

$$h_f = \frac{\sqrt{1+8\,V_c/V_d}-3}{4(V_c/V_d-1)} \quad (6)$$

The procedure is judged to be satisfactory if measured values of h_f agree approximately with Equation (6), in which case the maximum capacity at a given rotor speed $(V_d)_{max}/uC_R$ is obtained from Equation (4) when h_f is substituted for h.

Several sets of data have been compared with the model; included are data for the toluene-water system in two column sizes, data from an earlier investigation (*20*) for the system kerosene-water-butylamine and for seven different geometries in a 16-in. diam. column, and data published by Logsdail, Thornton, and Pratt (*16*) for the toluene-water system and five sets of dimensions in a 3-in. diam. column and for four other liquid systems and one geometry. In several cases both directions of dispersion were studied, and three cases include data obtained during solute transfer.

Illustrative data for one liquid system will be given here. Figure 6 shows data for toluene dispersed in water in 6- and 42-in. diam. RDC's (units u and v, Table 1) and for several flow rates and phase ratios in each column size. Figure 7 gives data obtained during transfer of acetone or methyl ethyl ketone solute from toluene drops to water; the curve through the points is that for the case without mass transfer, taken from Figure 6. The data in the two figures cluster around a common curve, greatest scatter occurring for runs at low drop holdups. Curves representing the theoretical model are given for two values of d/d_{max} on Figure 6. The experimental curve exhibits a greater slope than does the theoretical model; a likely explanation is that the factor $\epsilon^{-2/5}$ in Equation (1) does not accurately describe the drop breakup process.

From these data plus other results not presented the authors conclude that the method outlined is valid for most scale-up problems, provided that pilot data, including drop holdup measurements, are obtained in a small RDC of suitable design, and that a sufficient range of rotor speed is specified for the commercial design. Scatter of data is worst and agreement with the model is poorest for systems with very low interfacial tension, for cases where the physical properties (or the drop holdup) change rapidly in the contact zone, and for cases where the internal geometry departs from normal practice (units e and f, Table 1). Pilot-scale data are required for most systems in which mass transfer occurs, since the characteristic drop

* Tabular material has been deposited as document 7081 with the American Documentation Institute, Photoduplication Service, Library of Congress, Washington 25, D. C., and may be obtained for $1.25 for photoprints or for 35-mm. microfilm.

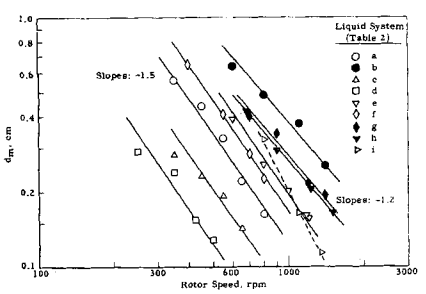

Fig. 2. Maximum stable drop size, 6-in. rotating disk contactor.

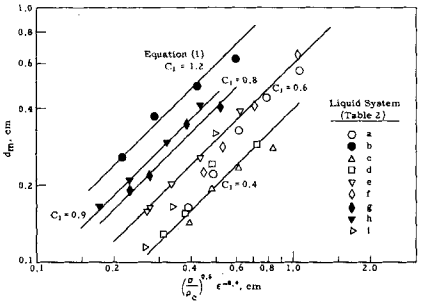

Fig. 3. Correlation of maximum stable drop sizes.

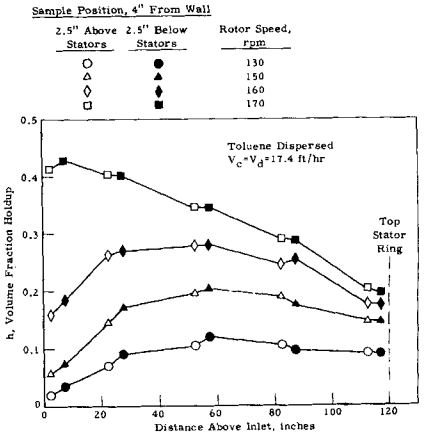

Fig. 4. Axial variation in dispersed-phase holdup, 42-in. diam. rotating disk contactor, toluene-water system.

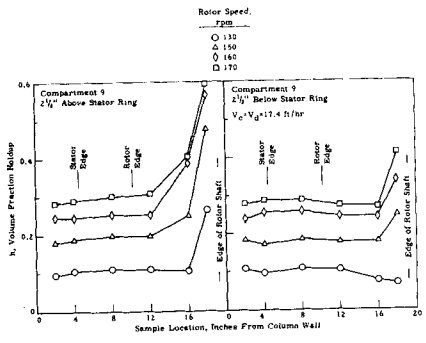

Fig. 5. Radial variation in dispersed-phase holdup, 42-in. diam. rotating disk contactor, toluene dispersed, water continuous.

size may depend quite strongly upon the transfer process. This results from the fact that mass transfer with the attendant change in interfacial properties may strongly inhibit drop coalescence in some cases, promote coalescence in others, and cause almost spontaneous emulsification in still other cases; such observations are now well documented (23, 26). These effects, when they occur, generally are functions of the solute concentration, and so holdup measurements may have to be made at several points along the length of the contactor when mass transfer is occurring.

A verification of the maximum holdup relation, Equation (6), is shown in Figure 8 for toluene dispersed in water and for the 42-in. diam. RDC. The agreement is considered to be satisfactory, in view of the difficulty of determining dispersed-phase holdup accurately at conditions approximately at or slightly above flooding. Other data, not shown, give about the same confirmation of the relation.

AXIAL MIXING

Two types of tests are required to define the axial mixing characteristics of an RDC. In the first, the eddy diffusion or backmixing characteristics are determined from tests in which a steady addition of tracer is made to the main flow in a compartment, and samples are taken from a compartment upstream after steady conditions are established. For this case the authors have obtained the backmixing or eddy diffusion coefficient E_b from the relation

$$E_b = \frac{VL}{\ln c_o/c} \qquad (7)$$

where c_o/c is the tracer concentration ratio existing over the axial distance $L = nH$.

Axial mixing which will be designated by the coefficient E_a, includes the eddy diffusion effect E_b as well as a spreading effect that is specific in the forward direction. The latter may be a channeling phenomenon or a

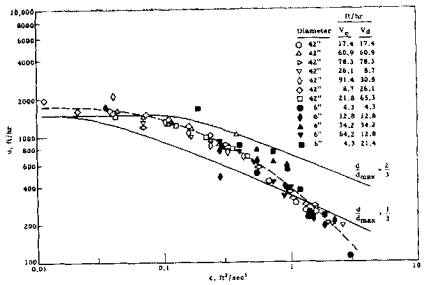

Fig. 6. Drop-velocity correlation, toluene dispersed in water, 6- (C_R = 0.450) and 42-in. diam. (C_R = 0.473) rotating disk contactors.

Taylor type of diffusion (27) peculiar to the particular geometry of the device. The procedure used to determine the total axial mixing effect is to inject a pulse of tracer at time zero and to sample downstream at subsequent times t. The authors have interpreted such data using the diffusion equation

$$E_a \frac{\partial^2 c}{\partial z^2} - V\frac{\partial c}{\partial z} = \frac{\partial c}{\partial t} \qquad (8)$$

with the boundary conditions for a semi-infinite strip

$$z = 0 \quad -E_a\frac{\partial c}{\partial z} + Vc = 0, \text{ for } t > 0$$

$$z \to \infty \quad c \to 0$$

for which the pulse-input solution is

$$\frac{c}{c_o} = \frac{1}{\sqrt{\pi}}\sqrt{\frac{VL}{E_a}\frac{\theta}{t}}\exp\left[-\left(\frac{VL}{4E_a}\right)\left(\sqrt{\frac{\theta}{t}} - \sqrt{\frac{t}{\theta}}\right)^2\right] - \frac{VL}{2E_a}e^{VL/E_a}$$

$$\text{erfc}\left[\sqrt{\frac{VL}{4E_a}}\left(\sqrt{\frac{\theta}{t}} + \sqrt{\frac{t}{\theta}}\right)\right] \qquad (9)$$

In some cases, depending upon the relative lengths of the test section and the over-all contact zone, the infinite-strip counterpart of Equation (9) has been used.

Both eddy diffusion and axial diffusion have been determined in several RDC's for the case where a single phase is flowing, and the continuous phase eddy diffusivity has been determined when two phases are present. In the latter case one finds that the appropriate Peclet number for eddy diffusion is $V_cL/E_b\ (1 - h)$, and one assumes the same form for axial mixing, that is $V_cL/E_a\ (1 - h)$. Only the axial diffusivity has been determined for the dispersed phase, and for this case the Peclet number is taken to be V_dL/hE_a. One recognizes that a description of the axial spreading of a drop population by a simple diffusivity E_a is subject to many limitations, since there are several phenomena that may affect the spread of residence times of a droplet phase in the presence of a counterflowing continuous phase. Among these are:

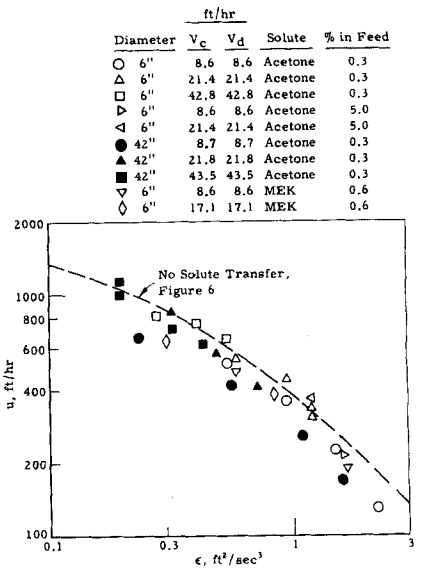

Fig. 7. Effect of solute transfer from toluene phase, toluene dispersed, water continuous.

1. Coalescence and breakup of drops.
2. Droplet velocity distribution due to different settling velocities of the various size fractions.
3. Droplet velocity distribution across the column radius due to vessel geometry and rotor speed.
4. Axial spreading of small drops due to turbulent velocity fluctuations in the continuous phase.

Therefore the correlation of E_a for the dispersed phase given here is intended only as a first attack on the problem, in order to obtain an approximate means of correcting mass transfer data for gross effects due to end-to-end mixing.

The authors will first consider the continuous phase data for E_b and E_a. Figure 9 shows the results of one retention-time-distribution run made in the 42-in. RDC and curves calculated from Equation (9); the authors would assign a diffusivity corresponding to $VL/E_a \cong 8$ for this run. Other runs have been analyzed in the same manner. The results for E_b and E_a for the 6-in. column are given in Figure 10, and similar results for the 42-in. column are given in Figure 11. One finds that a plot of E/VH against RN/V gives a unique correlation of the data for a given RDC, over a range of rotor speeds and flow rates. The shapes of the E_b and E_a curves are interesting. The curves tend to approach at high rotor speeds, which demonstrates that eddy diffusion is the dominant axial mixing process at such speeds. They diverge at lower speeds, and the E_a curves go through a minimum and finally to a somewhat higher plateau at very low speeds. This action, the authors think, indicates a channeling or Taylor-diffusion

effect peculiar to the RDC geometry. The fact that values of E_a/VS or E_a/VD from these data (at about zero rotor speed) agree approximately with E_a/VD values for pipe flow (*14, 29*) at about the same flow Reynolds number supports this view. The minimum in the E_a curve probably represents the competing effects of a radial diffusivity (which reduces channeling) and the eddy diffusivity E_b, as rotor speed is increased.

The eddy-diffusion data will not be considered further, since the authors' main interest here is in arriving at a correlation of E_a that is suitable for correcting column efficiency for the effects of axial mixing. The authors will consider only those E_a data for which $RN/V > 30$, since almost invariably one is not interested in mass transfer data obtained at still lower rotor speeds. As an aid in developing a correlation, resistance measurements were made in an electrical conductivity cell-analogue of an RDC, and these indicated that the resistance to current flow may be derived from series or series-parallel combinations of the dimensionless conductances: $(S/D)^2$, $1 - (R/D)^2$, $(S/D)^2 - (R/D)^2$, and $(H/D)[(S + R)/D]$. When one follows this lead, best success has been found using the groups

$$\frac{E_a}{VH} \text{ and } \left(\frac{RN}{V}\right)\left(\frac{R}{D}\right)^2 \left[\left(\frac{S}{D}\right)^2 - \left(\frac{R}{D}\right)^2\right]$$

The term in square brackets emphasizes the likelihood of channeling when S is much larger than R, but goes to zero, an unlikely limit, as $R \to S$. It is hoped that this deficiency can be corrected after more data are obtained.

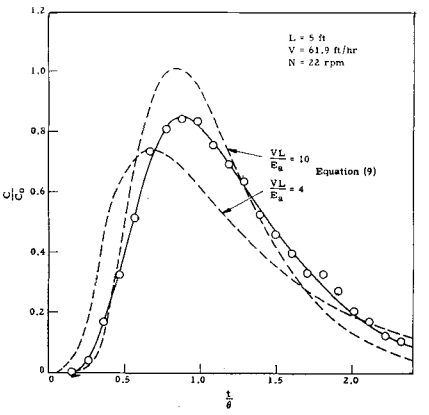

Fig. 9. Typical run, retention-time distribution, 42-in. diam. rotating disk contactor.

$$\frac{E_a}{VH} = 0.5 + 0.09\left(\frac{RN}{V}\right)\left(\frac{R}{D}\right)^2 \left[\left(\frac{S}{D}\right)^2 - \left(\frac{R}{D}\right)^2\right] \text{for } \frac{RN}{V} > 30 \quad (10)$$

Other data, not shown, for 25- and 85-in. diameter columns are correlated about as well. For the case where dispersed-phase flow is present one will take Equation (10) to be

$$\frac{(1-h)E_a}{V_cH} = 0.5 + 0.09\,(1-h)\left(\frac{RN}{V_c}\right)\left(\frac{R}{D}\right)^2\left[\left(\frac{S}{D}\right)^2 - \left(\frac{R}{D}\right)^2\right] \quad (11)$$

For dispersed phase axial mixing one assumes an analogous form; that is

$$\frac{hE_a}{V_dH} = 0.5 + 0.09h\left(\frac{RN}{V_d}\right)\left(\frac{R}{D}\right)^2\left[\left(\frac{S}{D}\right)^2 - \left(\frac{R}{D}\right)^2\right] \quad (12)$$

Equation (12) would be expected to best represent the situation at highest rotor speeds, since it has been shown that eddy diffusion dominates the axial mixing process at this condition, and since the low inertia of the small drops that are present at high speeds should cause them to follow the continuous-phase turbulent fluctuations. Figure 13 shows a test of Equation (12), with axial mixing data obtained in the 6-in. RDC for two sizes of solid particles settling in a continuous kerosene phase and for kerosene drops dispersed in water. The latter system is one for which little or no drop coalescence is seen to occur in the contact zone. The agreement with Equation (12) is only fair, but nevertheless the authors will use this equation in the present analysis. Further work, especially in conjunction with drop-size distribution and drop-interaction studies, may reveal a better approach to the problem of dispersed phase axial mixing.

EDDY DIFFUSION-MASS TRANSFER MODEL

The plug-flow equation for mass transfer generally is used to calculate the efficiency of a countercurrent-flow device; that is

$$T_p = \frac{1}{F-1}\ln_e\frac{1-\Psi_p}{1-F\Psi_p} \quad (13)$$

When axial mixing exists in the device, this equation obviously does not describe the true mass transfer conditions but merely gives the effective or apparent number of transfer units corresponding to the specific experiment and column dimensions. Application of this T_p to another operating condition or to another column size may give very erroneous results if the axial mixing effect is large. As an example, if T_p is determined for a short section of length L_1, then the number of transfer units that will be achieved in a long section of length L_2 with axial mixing present is not correctly given by $(T_{p1})(L_2/L_1)$.

The solution of the problem for mass transfer between the phases in a continuous column, with eddy diffusion present in both phases, has been given by Sleicher (*24*) and by McMullen, Miyauchi, and Vermeulen (*17*). The authors will use the Sleicher solution and will make the assumption that the axial diffusivities given here may be used as the eddy diffusivities that appear in his model. For the condition that $\Psi_p = \Psi$, his solution is given approximately by

$$\frac{T_p}{T} = \frac{N_{Pe_f}N_{Pe_s}}{N_{Pe_f}N_{Pe_s} + T_p[aN_{Pe_f} + bN_{Pe_s} + c\sqrt{N_{Pe_f}N_{Pe_s}} - d\sqrt{N_{Pe_f} + N_{Pe_s}} + f(N_{Pe_f} - N_{Pe_s})\,e^{-gT}]} \quad (14)$$

where T_p is given by Equation (13), and the coefficients $a, b, c \ldots\ldots$ are tabulated as functions of F by Sleicher (*24*). Equation (14) is most convenient for the case that T is known and

Figure 12 shows a test of the relation, with E_a data for single-phase flow obtained in 6- and 42-in. diam. units. The curve through the data is given by

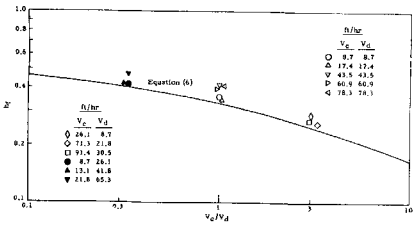

Fig. 8. Volume fraction holdup at flooding rotor speed, toluene dispersed in water, 42-in. diam. rotating disk contactor.

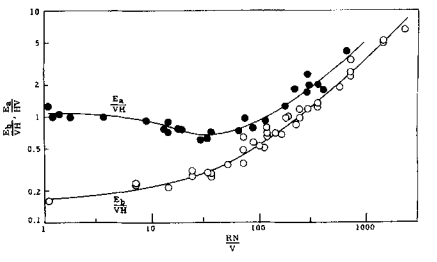

Fig. 10. Eddy diffusion and axial diffusion in 6-in. diam. rotating disk contactor.

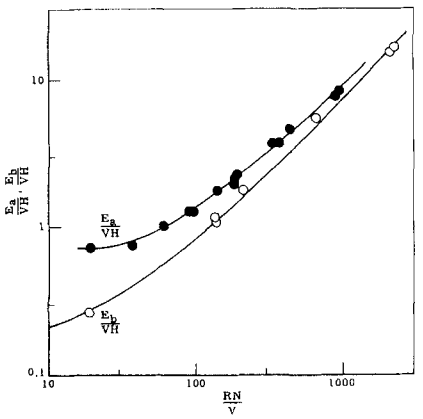

Fig. 11. Eddy diffusion and axial diffusion in 42-in. diam. rotating disk contactor.

T_p is sought. For the opposite case where T_p is known and T is wanted

$$\frac{T}{T_p} = \frac{N_{Pe_f}N_{Pe_s}}{N_{Pe_f}N_{Pe_s} - T_p[aN_{Pe_f} + bN_{Pe_s} + c\sqrt{N_{Pe_f}N_{Pe_s}} - d\sqrt{N_{Pe_f} + N_{Pe_s}} + f(N_{Pe_f} - N_{Pe_s})\,e^{-gT}]} \tag{15}$$

T_p is calculated from Equation (13) for the measured Ψ_p and given F and L, and T is then obtained from Equation (15) with this value of T_p and the appropriate values of N_{Pe_f} and N_{Pe_s}. A trial value of T in the term e^{-gT} is required, but generally this term is not very important in the summation. It will be noted that $T > T_p$ whenever axial mixing is present, that is when N_{Pe_f} and N_{Pe_s} are less than ∞. For simplicity in further discussions the authors will use the apparent transfer coefficient $(Ka)_p$, corresponding to T_pV_f/L, and the true transfer coefficient Ka, corresponding to TV_f/L.

When the feed phase is the dispersed phase, the over-all Peclet numbers are given by

$$N_{Pe_f} = \frac{V_dH}{hE_a}\frac{L}{H} \qquad N_{Pe_s} = \frac{V_cH}{(1-h)E_a}\frac{L}{H} \tag{16}$$

and for solvent dispersed

$$N_{Pe_f} = \frac{V_cH}{(1-h)E_a}\frac{L}{H} \qquad N_{Pe_s} = \frac{V_dH}{hE_a}\frac{L}{H} \tag{17}$$

where $(1-h)E_a/V_cH$ and hE_a/V_dH are obtained from Equations (11) and (12).

TYPICAL MASS TRANSFER DATA

The experimental results for the system toluene-water-acetone solute in 6- and 42-in. RDC's and for toluene-water-methyl ethyl ketone solute in a 6-in. unit are given in Table 4.* The apparent transfer coefficients $(Ka)_p$ as well as the true ones Ka are listed, where Ka has been obtained by the methods described in the previous section. It should be mentioned that the stator opening S/D in the 42-in. diam. unit (unit v, Table 1) is larger than that normally installed, to purposely emphasize the axial mixing effect.

Figure 14 shows the true number of transfer units per foot of column height Ka/V_f as a function of power/mass for these two systems. Figure 15 shows similar data for n-butylamine extraction from kerosene with water (kerosene-phase dispersed) in 4- and 16-in. diam. units and for five internal configurations in the 16-in. column (*20*). The corrected data are approximately independent of column length, diameter, and internal dimensions, the largest deviations occurring for internal dimensions that are outside the range normally used. Other data that will be discussed later, including those of Logsdail, Thornton, and Pratt (*16*), show approximately similar effects. Therefore the correction procedure, although it involves a number of assumptions and calculation steps, apparently gives a normally sufficient correction for flow imperfections due to column dimensions. Some exceptions with respect to very short columns are noted later.

The slopes of the curves on these figures are in the range of 0.7 to 1.0. This has no fundamental significance until so proved, since one is dealing with over-all coefficients, but it does indicate that one must search for a mechanism that allows an effect on Ka of approximately $\epsilon^{0.8}$ (or $N^{2.4}$ for a given design).

ANALYSIS OF MASS TRANSFER DATA

The elimination of the major effects due to column dimensions by the methods just discussed has encouraged the authors to think that the Ka's so calculated represent the true transfer conditions in the vicinity of a drop. Therefore the data just presented as well as Ka's from other studies in which drop holdup was determined (*16, 20, 32*) have been analyzed in terms of two limiting transfer mechanisms:

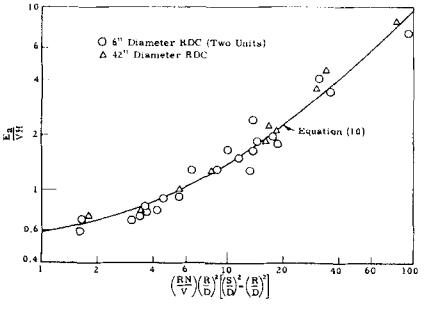

Fig. 12. Axial diffusion, single-phase flow, $RN/V > 30$.

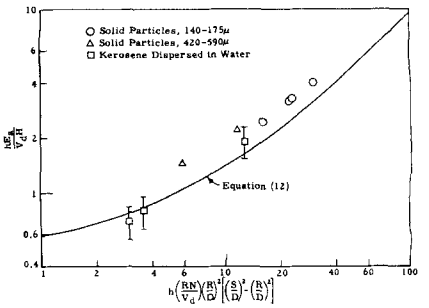

Fig. 13. Dispersed-phase axial diffusion, 6-in. diam. rotating disk contactor.

1. Transfer by molecular diffusion from stagnant drops and with an appropriate continuous-phase coefficient corresponding to inert drop behavior. For the latter one uses a Reynolds type of skin friction-mass transfer analogy [Equation (19)], where the constant is determined from the data. The over-all coefficient for this case is designated K_{SD}.

2. Transfer from circulating, oscillating drops, with a Higbie type of equation for the outside coefficient. This is the model proposed by Handlos and Baron (*6*), but for consistency the authors have added the stagnant drop coefficient (k_{iSD}) to their k_i. The over-all coefficient for this case is called K_{CD}.

For the stagnant drop model one obtains k_{iSD} from the Newman relation

$$e^{-(k_ia)_{SD}t/h} = \frac{6}{\pi^2}\sum_{n=1}^{\infty}\frac{1}{n^2}e^{-4\pi^2n^2\mathcal{D}_it/d^2} \tag{18}$$

and for k_{oSD} one takes

$$(k_o)_{SD} = 0.001u^* \tag{19}$$

Equation (18) is only an approximation when a continuous film resistance is present; various workers, for example (*30*), have pointed out its limitations. An exact solution for this case is available by analogy to the work of Munro and Amundson (*18*) involving heat transfer between counter-flowing gas and pebbles. Unfortunately this solution is too complicated to be readily applied here. Consequently one will use equation (18) despite its limitations.

For the circulating drop model one has (*6*)

$$(k_i)_{CD} = \frac{0.00375u^*}{1+\frac{\mu_i}{\mu_o}} + (k_i)_{SD} \tag{20}$$

$$(k_o)_{CD} = \sqrt{\frac{4}{\pi}}\sqrt{\frac{\mathcal{D}_ou^*}{d}} \tag{21}$$

Here $\mathcal{D}_i$ and $\mathcal{D}_o$ are the solute diffu-

* See footnote on page 255.

sivities in the drop phase and in the continuous phase, estimated via the Wilke-Chang correlation (33); $t = Lh/V_d$ is the drop contact time; μ_i and μ_o are the inside and outside phase viscosities; and the relative drop velocity u^* is defined by

$$u^* = \frac{V_d}{h} + \frac{V_c}{1-h} \qquad (22)$$

Over-all coefficients K_{SD} and K_{CD}, based on the feed phase in all cases, are obtained from these equations with the concept of additivity of resistances; for the feed phase dispersed one has

$$\frac{1}{K_f} = \frac{1}{K_i} = \frac{1}{k_i} + \frac{m}{k_o} \qquad (23)$$

and for solvent phase dispersed

$$\frac{1}{K_f} = \frac{1}{K_o} = \frac{1}{k_o} + \frac{m}{k_i} \qquad (24)$$

Table 5* lists the properties of the liquid system used in the calculations. Values of u [Equation (4)] were calculated with the experimental values of h, and d was then obtained for each run from a curve of d vs. u, constructed from the drop settling relation; alternatively, for some systems d was obtained from Equation (1) with an average value of C_1. Typical or average values of C_1 for all of the systems are given in Table 5.* The relative velocity u^* was obtained from Equation (22), and interfacial area a was determined on the assumption that spherical drops are present; that is

$$a = 6\,h/d \qquad (25)$$

Thus one obtains the experimental K from Ka/a.

For simplicity in presentation the authors show the ratios K/K_{SD} and K_{CD}/K_{SD} for each liquid system as functions of the dimensionless modulus $du^*/\mathcal{D}_i$; this permits seeing directly the position of the experimental K's relative to the calculated K_{SD} and K_{CD}. This method of plotting is essentially correct for long contact times and small drops but becomes poorer when the inequality

$$4\pi^2\mathcal{D}_i/d >> \frac{d}{t}\ln\frac{\pi^2}{6} \qquad (26)$$

is no longer met. For this reason the authors have arbitrarily divided the data into those for long column sections and those for short sections, and the data will be discussed in this sense.

Figures 16 and 17 show comparisons for three different liquid systems and for various column diameters, lengths, and internal dimensions. The conditions used in each study are shown on the figures or may be obtained by referring to Tables 1 and 5.* The runs for all rotor speeds, flow rates, and flow ratios are included, except that runs for which h was less than about 0.02 or greater than the estimated h_f, or for which $(T/T_p) \tilde{>} 5$ have been rejected. The data from additional studies are summarized in Table 6;* the ratios K/K_{SD} and K_{CD}/K_{SD} are listed for only two values of $du^*/\mathcal{D}_i$, but this is sufficient to orient one as to the shape of the curves. A residual effect of rotor speed is found in only one case [Vermijs and Kramers (32), Table 6*] which may be the result of using a comparatively low peripheral speed in a small diameter.

The scatter of data in some of the comparisons is greater than one likes to see, but a certain scatter is inevitable since five computations are required to obtain K from Ψ_p, and since nine separately determined quantities (Ka, N, V_d, V_c/V_d, ϵ, m, h, d, and u^*) enter into the calculations.

The plots of K/K_{SD} vs. $du^*/\mathcal{D}_i$ are essentially independent of column size effects; exceptions to this, for rather unusual geometries, are seen in Figure 17, Table 6,* reference *16*. Also some exceptions are found between the data for short and long sections, for a given liquid system. One example is the toluene-water-acetone system, Figure 16, Table 6,* reference *16*; this case and others will be discussed in a later paragraph.

The two systems that exhibit the most extreme behavior are toluene-water-acetone, Figure 16, for which K is of the order of K_{SD}, and methyl isobutyl ketone-water-acetic acid, Table 6,* for which K is of the order of K_{CD}. Three observations cited earlier support the idea that the drops for the first system are relatively inert: transfer of acetone has little effect on drop holdup, the relation between u and ϵ is little affected by acetone transfer, and acetone concentrations of 0.2 to 5.0% in the feed have little effect on the transfer coefficient. The methyl isobutyl ketone-water-acetic acid system has long been known as one that is easy to extract and has been used in many studies. The authors' data for this system show considerable scatter, perhaps indicative of drop interaction, and show an appreciable effect due to solute concentration. The other liquid systems fall more or less between these two systems.

The indication that drop behavior may range from static to very mobile is not surprising, in view of similar findings reported for some single-drop studies [see for example Johnson and Hamielec (*10*)]. This means that column design in the absence of pilot-scale efficiency data can be quite uncertain, unless one takes the conservative (K_{SD}) basis. The same uncertainty probably holds for other extraction devices. Moreover K_{SD} may not be so conservative for plant streams in which trace materials may inhibit drop circulation, or for devices in which the drop size is very small. With regard to the latter point the analysis by Treybal (*30*) and by Olney (*19*) of various stirred-vessel data suggests that mass transfer in stirred tanks frequently is limited by molecular diffusion or by slow circulation in the drops.

* See footnote on page 255.

* See footnote in column 1.

* See footnote in column 1.

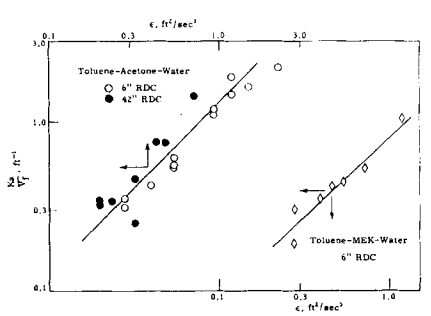

Fig. 14. True mass transfer coefficients, data from Table 5.

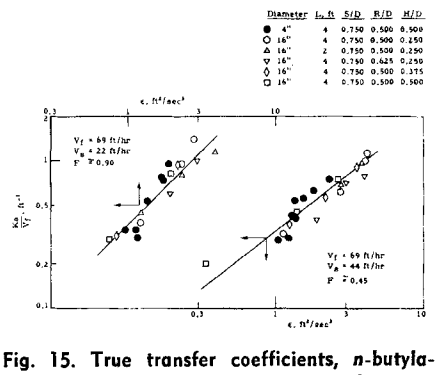

Fig. 15. True transfer coefficients, *n*-butylamine transfer from kerosene to water, kerosene dispersed (*20*).

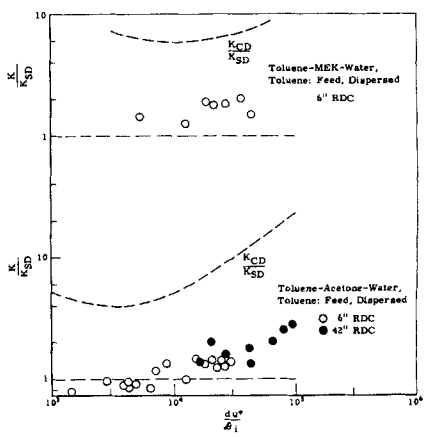

Fig. 16. Toluene-water-solute systems, data from Table 5.

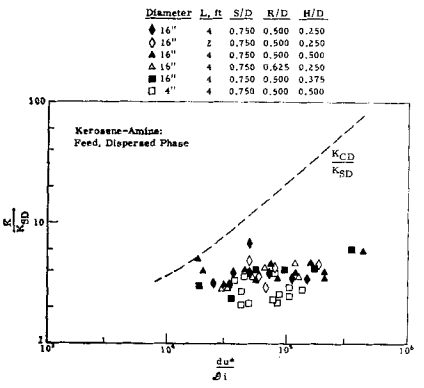

Fig. 17. Kerosene-*n*-butylamine-water system, 4- and 16-in. diam. rotating disk contactors, reference 20.

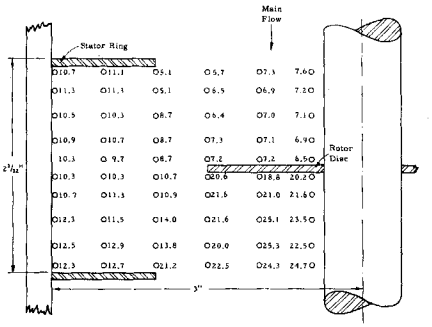

Fig. 18. Point-tracer concentrations in a rotating disk contactor compartment, for $RN/V = 117$.

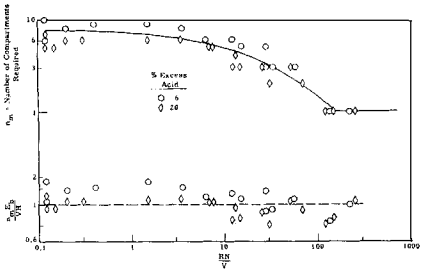

Fig. 19. Molecular mixing times in 6-in. diam. rotating disk contactor.

As already mentioned the acetone transfer rates from toluene drops to water are higher in the 3 in × 2 ft. unit studied by Logsdail (*16*) than in the authors' studies in 6 in. × 6 ft. and 42 in. × 10 ft units. Also, the transfer of acetic acid from water drops to methyl isobutyl ketone is slower in the 1.6 in. × 1.55 ft RDC used by Vermijs and Kramers (*32*) than in the 4 in. × 4 ft unit used by the authors. These differences may be due to the presence of trace contaminants in one case and not in the other, or to inlet effects, probably most pronounced in the short columns, or because ultimate drop behavior is not established in a short contact time. The three indications from the authors' work that acetone transfer has little effect on the behavior of toluene drops have already been mentioned; in contrast Logsdail et al. find that acetone transfer from the toluene drops causes a significant increase in the flooding rates attainable. The cause of these differences cannot now be isolated, but the results emphasize the need for maintaining similar extraction severities and the same bulk and interfacial properties in two equipment scales, in order to determine the true effect of equipment size on the result.

In general one finds that a plot of K, K_{SD}, and K_{CD} vs. $du^*/\mathcal{D}_i$ provides a better basis for interpolating and extrapolating RDC pilot data than do more pragmatic methods. Also the method generally requires a smaller number of pilot runs for a safe plant design. Good measurments of drop holdup cannot be made in some process studies, of course, and for these cases other scale-up procedures are used (*20, 22*).

MISCELLANEOUS STUDIES

Point tracer concentrations, determined at various positions within an RDC compartment during steady state backmixing tests, provide a description of the nature of the flow patterns within a compartment. Figure 18 shows the concentrations determined in one compartment of the 6-in. RDC, several compartments upstream of the tracer (dye) injection point. A relatively well-mixed zone exists in the outer annulus between adjacent stator rings, and another uniform zone exists in the center core between adjacent rotor disks. A large concentration gradient exists across the small region between these zones. This gradient is a function of the rotor speed, flow velocity, and compartment dimensions, and it defines the region of main resistance to back diffusion. A similar description of the flow patterns has been obtained in the 42-in. diam. column, and an indication of similar patterns is found in some of the work of Kung and Beckmann (*13*).

The use of an RDC as a reactor for homogeneous liquid-phase reactions has been considered from time to time. Some of the potential advantages are compact dimensions, acceptable axial diffusion rates when residence time is not extremely long, good wall heat transfer coefficients, and rapid blending of reactants. The latter requirement may arise for example if one or more additions of a reactant are made along the length of a reactor and if rapid mixing, on a molecular scale, of these additions with the main stream is required to minimize yield losses. Some experiments to determine this mixing time have been done in the 6-in. RDC; a side stream of acid (sulfuric acid) was injected continuously at one compartment into the main stream flow (sodium hydroxide solution containing phenolphthalein indicator), and the mixing time was determined by observing the compartment downstream in which the indicator changed color. Various flow rates and rotor speeds were tried, and two acid concentration levels (6 and 20% excess) were used in order to give an impression of the mixing times required for an equal concentration of ionic species. Figure 19 gives the results, where n_m is the number of compartments required for mixing, and VH/E_b is the Peclet number for eddy diffusion, which was discussed earlier. The fact that the ratio n_mE_b/VH is found to be of the order of unity indicates that the mixing process and the eddy diffusion process are superficially the same in an RDC. Using certain assumptions one can show theoretically that a proportionality between n_m and VH/E_b is to be expected. The authors take the mixing time θ_m in a homogeneous turbulence to be

$$\theta_m = \tau \frac{l_o}{U_o} \qquad (27)$$

Also one may define the eddy diffusivity as

$$E_b = C_3 l_o U_o \qquad (28)$$

If one takes $\theta_m = n_mH/V$ and eliminates U_o from Equations (27) and (28), one finds

$$n_m = C_{3\tau} \left(\frac{l_o}{H}\right)^2 \frac{VH}{E_b} \qquad (29)$$

A reasonable value for $\tau(1)$ is thought to be about 10, for liquids of Schmidt number $\cong$ 500, and $H/3$ is a reasonable limit for l_o since the internal geometry restricts l_o to a maximum value of about $H/2$. If one further assumes that $C_3 \cong 1$ in Equation (28), then $C_{3\tau}(l_o/H)^2$ is of the order of unity and the approximate equality between n_m and VH/E_b found in Figure 19 is indicated.

The actual mixing times found in the 6-in. RDC range from a low of about 1.2 sec. for N = 1,400 rev./min. and V = 1,700 ft./hr. to a high of 2.7 min. at $N \cong 0$ and V = 27 ft./hr. When a pulse of acid was added the mixing process was seen to proceed by jumps of axial dimension $H/2$, which is consistent with the above concepts and with the flow description provided by Figure 18.

DISCUSSION

The work reported indicates that certain two-phase contactors can be analyzed with first principles for the main framework of the analysis. Some

refinements in the methods are desirable, and work is continuing on these.

The separation of local mass transfer effects from gross mixing effects has been demonstrated, and it is hoped that this result will encourage others to try similar procedures for other types of two-phase contactors. Finding that the two limiting transfer mechanisms approximately define the range of experimental transfer rates confirms the earlier observations of others. This result emphasizes that a knowledge of the behavior of drops and interfaces under transfer conditions is essential in predicting the performance of practical devices. Other areas of fundamental and practical interest for further study pointed up by the work include a description of the drop breakup process in a turbulence, that gives the distribution of drop sizes typically found in flow contactors; the nature of the eddy motions of a swarm of drops in countercurrent flow apparatus; and the rates of interaction (repeated coalescence and breakup) of a drop population in a dynamic environment.

ACKNOWLEDGMENT

The authors acknowledge the valuable contributions of several colleagues, particularly D. B. Todd, C. A. Sleicher, and H. A. Wistrich.

NOTATION

a = interfacial area per unit volume of tower

c = tracer concentration; c_o = inlet or initial tracer concentration

C_1 = dimensionless coefficient in drop breakup equation

C_2 = dimensionless coefficient in power number

C_3 = coefficient in Equation (28)

C_R = constriction area ratio, defined by Equation (5)

d = drop diameter; d_m = maximum stable drop size

D = column diameter

$\mathcal{D}$ = molecular diffusivity of solute

E_a = axial diffusion coefficient; E_b = eddy diffusion coefficient

F = extraction factor, mV_f/V_s

g = acceleration of gravity

g_c = conversion factor, (ft./sec.^{2}) (lb. mass/lb. force)

h = volume fraction holdup of drop phase; h_f = maximum holdup

H = compartment height

k_i = drop phase film coefficient; k_o = outside film coefficient

K = over-all mass transfer coefficient, based on feed phase

l_o = scale of largest turbulent eddies

L = total length of contact zone; length between injection and sampling points

m = distribution coefficient, (wt. solute/vol. feed)/(wt. solute/vol. solvent)

n = number of compartments; n_m = number of compartments required for mixing on a molecular scale

N = rotor disk speed, rev./time

N_{Pe_f} = over-all Peclet number for feed phase; N_{Pe_s} = over-all Peclet number for solvent phase

P = net power input

R = rotor disk diameter

S = stator ring opening

t = time

T = number of over-all transfer units based on feed phase, KaL/V_f; T_p = T for plug-flow conditions

u = characteristic drop velocity, defined by Equation (4); u^* = relative drop velocity, defined by Equation (22)

U_o = root-mean-square fluctuating velocity

V = superficial velocity, single phase flowing; V_c = same, continuous phase; V_d = same, dispersed phase; V_f = same, feed phase; V_s = same, solvent phase; $(V_d)_{max}$ = superficial velocity of dispersed phase at flooding or at maximum holdup

x_o = solute concentration in feed; x_1 = solute concentration in raffinate

y_o = solute concentration in entering solvent

z = length variable

Greek Letters

ϵ = power per unit mass, defined by Equation (2)

θ = average residence time; θ_m = time for molecular mixing to occur

μ = viscosity; size, micron

ρ = density; $\bar{\rho}$ = average density, $h\rho_d + (1 - h)\rho_c$

σ = interfacial tension

τ = dimensionless time defined by Equation (27)

Ψ = $(x_o - x_1)/(x_o - my_o)$; Ψ_p = Ψ for plug-flow conditions

Subscripts

c,o = continuous or outside phase

d,i = dispersed or inside phase

CD = circulating, oscillating drop model

f = feed phase

s = solvent phase

SD = stagnant drop model

LITERATURE CITED

1. Beek, J., and R. S. Miller, *Chem. Eng. Progr. Symposium Ser. No. 25*, **55**, 23 (1959).
2. Calderbank, P. H., and I. J. O. Korchinsky, *Chem. Eng. Sci.*, **6**, 65 (1956).
3. Calderbank, P. H., *Trans. Inst. Chem. Engrs.*, **36**, 443 (1958).
4. Clay, P. H., *Proc. Roy. Acad. Sci. (Amsterdam)*, **43**, 852, 979 (1940).
5. Dittman, J. G., Paper presented at Am. Inst. Chem. Engrs. meeting, San Francisco, California (December, 1959).
6. Handlos, A. E., and Thomas Baron, *A.I.Ch.E. Journal*, **3**, 127 (1957).
7. Hinze, J. O., *ibid.*, **1**, 289 (1955).
8. Hu, Shengen, and R. C. Kintner, *A.I.Ch.E. Journal*, **1**, 43 (1955).
9. Hughes, R. R., and E. R. Gilliland, *Chem. Eng. Progr.*, **48**, 497 (1952).
10. Johnson, A. I., and A. E. Hamielec, *A.I.Ch.E. Journal*, **6**, 145 (1960).
11. Kafarov, V. V., and B. M. Babanov, *J. Appl. Chem. (USSR)*, **32**, 810 (1959).
12. Kolmogorov, A. N., *Doklady Akad. Nauk (USSR)*, **66**, 825 (1949).
13. Kung, E. Y., and R. B. Beckmann, *A.I.Ch.E. Journal*, **7**, No. 2 (1961).
14. Levenspiel, O., *Ind. Eng. Chem.*, **50**, 343 (1958).
15. Licht, William, and G. S. R. Narasimhamurty, *A.I.Ch.E. Journal*, **1**, 366 (1955).
16. Logsdail, D. H., J. D. Thornton, and H. R. C. Pratt, *Trans. Inst. Chem. Engrs.*, **35**, 301 (1957).
17. McMullen, A. K., T. Miyauchi, and Theodore Vermeulen, *UCRL-3911*, Supplement, U.S. Atomic Energy Comm. (1958).
18. Munro, W. D., and N. R. Amundson, *Ind. Eng. Chem.*, **42**, 1481 (1950).
19. Olney, R. B., *A.I.Ch.E. Journal*, **7**, No. 2 (1961).
20. Reman, G. H., and R. B. Olney, *Chem. Eng. Progr.*, **51**, 141 (1955).
21. Reman, G. H., and J. G. van de Vusse, *Génie chim.*, **74**, 106 (1955).
22. Reman, G. H., "Joint Symposium, Scaling-Up Chem. Plant and Processes," p. 26, Institution of Chemical Engineers, London, England (1957).
23. Sherwood, T. K., and J. C. Wei, *Ind. Eng. Chem.*, **49**, 1030 (1957).
24. Sleicher, C. A., *A.I.Ch.E. Journal*, **5**, 145 (1959).
25. Sleicher, C. A., *ibid.*, to be published.
26. Sternling, C. V., and L. E. Scriven, *ibid.*, **5**, 514 (1959).
27. Taylor, G. I., *Proc. Roy. Soc (London)*, **A219**, 186 (1953).
28. Thornton, J. D., *Chem. Eng. Sci.*, **5**, 201 (1956).
29. Tichacek, L. J., C. H. Barkelew, and Thomas Baron, *A.I.Ch.E. Journal*, **3**, 439 (1957).
30. Treybal, R. E., *ibid.*, **4**, 202 (1958).
31. Vermeulen, Theodore, G. M. Williams, and G. E. Langlois, *Chem. Eng. Progr.*, **51**, 85 (1955).
32. Vermijs, H. J. A., and H. A. Kramers, *Chem. Eng. Sci.*, **3**, 55 (1954).
33. Wilke, C. R., and Pin Chang, *A.I.Ch.E. Journal*, **1**, 264 (1955).

Manuscript received September 20, 1960; revision received October 10, 1961; paper accepted October 11, 1961. Paper presented at A.I.Ch.E. New Orleans meeting.